

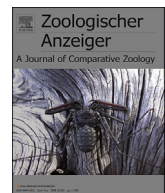


ELSEVIER

Contents lists available at ScienceDirect

Zoologischer Anzeiger

journal homepage: www.elsevier.com/locate/jcz



Research paper

Integration of morphological and molecular taxonomic characters for identification of *Odontoponera denticulata* (Hymenoptera: Formicidae: Ponerinae) with the description of the antennal sensilla

Hridisha Nandana Hazarika, Bulbuli Khanikor*

Department of Zoology, Gauhati University, Guwahati, 781014, Assam, India



ARTICLE INFO

Article history:

Received 16 March 2020

Received in revised form

25 May 2021

Accepted 26 May 2021

Available online 1 June 2021

Corresponding Editor name: Sven Bradler

Keywords:

Antennal sensilla

DNA barcoding

Morphology

Odontoponera

ABSTRACT

Integration of morphological and molecular approaches is nowadays given importance to identify a particular species. So in our study, we considered both approaches to identify the controversial ant species, *Odontoponera denticulata*. For morphological analysis, we considered morphological characters and morphometric measurements. In the molecular approach, we considered DNA barcoding from the COI gene. A nucleotide sequence of 641 base pairs was obtained which showed 86.08% similarity with *Odontoponera transversa*. No COI gene sequence of *O. denticulata* is found to exist in Genbank. But morphological characters supported the identity of the species as *O. denticulata*. Therefore, the sequence obtained was submitted to NCBI Genbank (accession number MN380424). From the study, it can be inferred that the combination of both the morphological and molecular approaches is helpful to identify a species, here in this case the Ponerine ant, *O. denticulata*. As there is no report on antennal sensilla of *O. denticulata*, therefore we also investigated the morphology and distribution of antennal sensilla of *O. denticulata*. Nine different types of antennal sensilla are recorded including Böhm Bristles (BB1, BB2), Sensilla Trichodea (ST1, ST2), Sensilla Chaetica (SCh), Sensilla Basiconica (SB1, SB2), Sensilla Coeloconica (SCo) and Sensilla Campaniformia (SCa). ST1 is the most abundant antennal sensilla found in *O. denticulata*.

© 2021 Elsevier GmbH. All rights reserved.

1. Introduction

Odontoponera is a small genus of subfamily Ponerinae under the family Formicidae. This genus is represented by only two extant species namely *O. denticulata* and *O. transversa*. The term “*Odontoponera*” was first coined by Mayr in 1862 for the ant species *Ponera denticulata* (F. Smith). Later, Dalla Torre (1893) synonymized *O. denticulata* with *O. transversa* (F. Smith). This was the starting point of taxonomic confusion which was followed by various authors for a long time (Santschi 1920; Creighton 1929; Bolton 1995; Bharti 2008; 2011; Bharti et al. 2013). However, Yamane (2009) separated *O. denticulata* from the *O. transversa* and described *O. denticulata* as a different species with their distinguishing characters such as relatively shorter antennal scape, generally passing the posterior margin of the head by less than a length of the first

funicular segment; comparatively larger eye, the minimum distance between the anterior margin of the eye and the anterior margin of the gena to the maximum length of the eye ranges from 1.2 to 1.4 in worker; development of less defined raised area on the vertex of the head, condition of rugae on the mesosoma, long and dense pilosity on the subpetiolar process; more than two larger teeth present in propodeum and body colour much darker with reddish legs.

Identification of an organism up to the species level is a difficult task and it requires specialized knowledge (Monaghan et al. 2005). Using only a single taxonomy approach i.e. either morphological or molecular approaches has faced criticism in the identification of species (Knowlton 1993; Jarman & Elliott 2000; Rubinhoof 2006). Therefore, the incorporation of both morphological and molecular approaches leads to taxonomic constancy (Padial et al. 2010).

As molecular approach DNA barcoding is a very effective tool for species identification of insects (Kumar et al. 2012), it contributes a new direction for species-level identification among invertebrates and vertebrates (Hebert et al. 2004; Hajibabaei et al. 2006). DNA barcoding is the DNA sequence analysis of a short (between 600

* Corresponding author.

E-mail addresses: hnhazarika4@gmail.com (H.N. Hazarika), bkz11@gauhati.ac.in (B. Khanikor).

and 900bp) standard segment of the genome (Hebert et al. 2003a). Barcode regions for identification of different organisms vary such as ITS (Internal Transcribed Spacer), rRNA gene, RuBisco gene, 16S rRNA gene, 18S rRNA gene, COI gene. For the identification of animals commonly mitochondrial gene cytochrome C oxidase (COI) is used as the barcode region. Although at a higher taxonomic level mitochondrial genes are not suitable for phylogenetic reconstruction (Waugh 2007), compared to the nuclear genome they have a high mutation rate, high degrees of intraspecific polymorphism and divergence. Therefore mitochondrial genes are good markers for species-level differentiation and evolutionary studies (Williams & Knowlton 2001; Wheat & Watt 2008; Hlaing et al. 2009). This region also possesses enough sequence variation to discriminate most animal species (Hajibabaei et al. 2006; Hebert et al. 2003b), therefore in animals, part of the mitochondrial gene COI is suitable as a DNA barcode region.

In addition to this, insect sensilla are basic structural and functional sensory units of the cuticle with mechano and chemoreceptor functions (Chapman 1998). In the order Hymenoptera, various sensilla were investigated with respect to the organization of the nervous system, nestmate discrimination and host preference behaviour (Ozaki et al. 2005; van Baaren et al. 2007; Nishino et al. 2009). Sensilla are present in different body parts of insects but mainly on antennae and mouthparts (De Facci et al. 2011). Based on their morphology (i.e., pores and wall properties), sensilla are classified into various types such as sensilla trichodea, sensilla basiconica, sensilla chaetica, sensilla coeloconica, sensilla placodea, sensilla ampullacea, sensilla campaniformia (Keil 1999; Nation 2002). They play an important role in gathering information from the environment ranging from odor, sound, heat, cold, humidity to tactile information and direct the insects to respond accordingly (Altner & Prillinger 1980; Chapman 1998). Several investigations of antennal sensilla in various ant species have been performed (Rental et al. 2003; Nakanishi et al. 2009; Babu et al. 2011), but no existing literature is available on the antennal sensilla of *O. denticulata*.

Thus, realizing the importance of both the molecular and morphological techniques we attempted both approaches for identification of the ponerine ant, *Odontoponera denticulata* with special emphasis on the morphology and distribution of antennal sensilla.

2. Materials and methods

2.1. Collection and preservation of samples

The ant samples were collected from Donduwa, Laokhowa Wildlife Sanctuary, Assam, India ($26^{\circ}29'N$, $92^{\circ}42'E$) and Kumardong, Kholahat Reserve Forest, Assam, India ($26^{\circ}07'N$, $92^{\circ}24'E$) using the standard protocol (Bharti et al. 2016) followed with modifications during 2018. The hand collection technique was carried out for the sampling of ants and 100 worker ants were collected from each study site. After the collection of the ant samples, they were washed in water and preserved in 99.9% ethanol.

2.2. Identification of ants based on morphological approach

Ants were identified based on the morphological characters of the worker caste. The collected ant samples were identified and photographed by using stereomicroscope (Leica EZE4) and Scanning Electron Microscope (ZEISS Sigma 300) based on identification key (Bolton 1994; Holldobler & Wilson 1990; Yamane 2007).

2.3. Scanning Electron Microscopy (SEM)

Freshly collected six workers were selected and their different body parts such as head, antennae, mesosoma, petiole and gaster were dissected under dissecting microscope. The sample preparation for SEM was done using the standard protocol (Hu et al. 2009) followed with modifications. The samples were dehydrated in a graded ascending alcohol series of 30%, 50%, 70%, 80%, 90% and 100% in each case for 15 min and cleared in acetone. After air dried, the prepared samples were then mounted on aluminum stubs with double-sided sticky carbon tapes. Then the samples were coated with gold in a (Quorum Q150R ES) high-resolution sputter coater. The samples were examined in a Scanning Electron microscope (Zeiss Sigma 300) present in the Central Instruments Facility (CIF), Gauhati University, Assam, India.

2.4. Morphological measurement and indices

For morphological measurement, six workers were selected. The morphological measurement and indices of ant workers were done using standard measurements given by Leong et al. (2017) with modifications.

2.4.1. Morphological measurements

Head Length (HL): It was measured from the anterior-most point of median clypeus margin to midpoint of occipital margin of the head in full-face view.

Head Width (HW): It was measured the maximum width of the head in full-face view excluding the compound eyes.

Scape Length (SC): It was measured the maximum length of the scape of antennae excluding the basal neck and condyle.

Antennae Length (AL): It was measured from condyle to the tip of the antennae.

Pronotal Width (PrW): It was measured the maximum dorsal width of the pronotum.

Weber's Length (WL): It was measured from anteriormost point of pronotum to posteriormost point of propodeum.

Mesosomal Length (ML): It was measured from the anterior edge of the pronotum excluding the collar to the posterior edge of the propodeal lobe.

Petiole Length (PL): It was measured from the anterior margin of the petiolar denticle to the posterior face of the petiole in lateral view.

Gaster Length (GL): It was measured from the base of the first gastral tergite to the apex of the gaster in lateral view.

Foreleg Length (FLL): It was measured from coxa to pretarsus of foreleg excluding claws.

Midleg Length (MLL): It was measured from coxa to pretarsus of midleg excluding claws.

Hindleg Length (HLL): It was measured from coxa to pretarsus of hindleg excluding claws.

Total Length (TL): It was measured from the tip of the mandible to the tip of the gaster excluding the sting.

2.4.2. Morphological indices

Cephalic Index (CI): $HW/HL \times 100$.

Scape Index (SI): $SL/HW \times 100$.

2.5. Identification of ants based on molecular taxonomy

The molecular taxonomy was done into the following steps-

2.5.1. DNA extraction, amplification and sequencing

Full genomic DNA was extracted from a pool of ants with five repetitions using QIAGEN kit, Blood and Tissue DNAeasy. We

amplified the 5' end of the Cytochrome Oxidase I (COI) gene using the forward and reverse primers respectively LCO1490(5'-GGTCAACAAATCATAAAGATATTGG-3') and HCO2198(5'- TAAACTTCAGGGTGACCAAAAAATCA-3') (Folmer et al. 1994). Polymerase chain reaction (PCR) amplifications were performed in a 25 μ L total volumes, which included 1 μ L of DNA, 2.5 μ L of 10X PCR buffer, 0.75 μ L of 50 mM MgCl₂, 0.5 μ L of 0.5 mM of dNTP mix, 0.5 μ L of 10 pmol primer solution, 0.5 μ L Taq DNA polymerase and 19.25 μ L nuclease-free water. PCR was performed with an initial denaturation of 5 min (95 °C) followed by denaturation of 1 min (94 °C), annealing of 1 min (45 °C), an extension of 90 s (72 °C) and a final extension of 7 min (72 °C). The amplified DNA fragments were run on a 2% agarose gel using ethidium bromide and visualized with a gel imaging system.

2.5.2. PCR product purification

Before the sequencing of PCR amplicons, unused dNTPs and primers were removed from the reaction mixture. The 10 μ L PCR product was used for ExoSAP purification. ExoSAP-IT™ PCR Product Cleanup chemical agent was used for accelerator cleanup of amplified PCR product by hydrolyzing excess primers and nucleotides. The advantage of adding ExoSAP-IT reagent directly to the PCR product is that it reduces the chances of cross-contamination and conserves PCR amplicons. 5 μ L of a post-PCR reaction product was mixed with 2 μ L of ExoSAP-IT reagent for the final reaction volume of 7 μ L. The reaction was incubated at 37 °C for 60 min to degrade the remaining primers and nucleotides and inactivated by incubation at 80 °C for 15 min. Then the PCR product was ready for use in DNA sequencing.

2.5.3. DNA sequencing of PCR products

DNA sequencing of PCR product was performed using Applied Biosystems BigDye Terminator V3.1 Cycle Sequencing kit. The sequencing products were loaded on Applied Biosystems 3130 Genetic Analyzer – an automated DNA sequencing machine. Sequences were analyzed using Sequencing Analysis 5.1 software available within the sequencing instrument. These sequences were further analyzed using ChromasPro v 1.34. Forward and reverse sequences were aligned to generate one contig with the best sequence.

2.5.4. Phylogenetic analysis

COI region sequences obtained from investigated ant samples were assembled using ChromasProV3.1 sequence assembly software. The assembled sequences were used for BLAST analysis using multiple sequence analysis tools available at the NCBI database. The reference sequences of the BLAST hit results were downloaded from the database. Then the reference sequences obtained from the NCBI Genbank database were annotated according to the alignment with the query sequences. Eighteen different ant species were selected from the BLAST results which show more than 81%–100% query cover for phylogenetic analysis and labelled with the accession number and the name of the ant species as it appears in the BLAST result. Clustal W online tool was used for the analysis of the phylogenetic relationship among the query and reference sequences. Then the alignment was converted in the MEGA format using MEGAX software. The phylogenetic tree was constructed by the neighbor-joining method (Saitou & Nei 1987) that applied to DNA distance matrices calculated according to the Kimura two-parameter model (Kimura 1980), and the confidence values of branches were determined by bootstrap analysis (500 replicates).

A phylogenetic tree based on COI region sequences for investigated ant species was constructed. Numbers at the various nodes were a percentage of 500 bootstrap replicates and the bar indicates genetic distance which arose due to sequence variation. Branches

matching the partitions reproduced in less than 50% bootstrap replicates were broken down and the percentage of replicate trees in which the associated taxa clustered together in the bootstrap test was shown next to the branches (Felsenstein 1985). The evolutionary distances were computed based on the Maximum Composite Likelihood method (Tamura et al. 2004). Codon positions included were 1st+2nd+3rd + Noncoding. All ambiguous positions containing gaps and missing data were further eliminated from the dataset.

2.6. Identification and distribution of antennal sensilla

Different types of sensilla present on the antennae of the investigated ant species were identified based on their morphological features defined in the existing literature (Schneider 1964; Zacharuk 1985). For counting the total number of antennal sensilla, the scape was divided into three regions-basal, median and proximal; pedicel and 10 flagellomeres. From each region of the antenna, a grid of 10000 μm^2 area was selected and counted the total number of sensilla. Means and Standard Errors were calculated using MS—EXCEL.

3. Results

3.1. Description of worker

The workers of *O. denticulata* are dark brown in colour and the legs are reddish in colour (Fig. 1). The total body length of the workers is measuring 10.35 ± 0.05 mm (Table 1). Head and mesosoma have cavernous rugae. In full-face view, the head is rectangular in shape (Fig. 2A), measuring the length of the head is 3.2 ± 0.03 mm and width is 2.81 ± 0.015 mm, the lateral sides of the head are somewhat convex, the occipital margin is even and the vertex has a poorly developed raised area near occipital margin (Fig. 3A). The cephalic index is 87.7 (Table 2). The anterior margin of the clypeus has longitudinal striae, pilosity present, containing eight teeth (Fig. 3B). Mandibles are strong, smooth, triangular in shape and contain five teeth (Fig. 2C). Compound eyes are large and circular in shape containing 195–205 numbers of ommatidia (Fig. 3C). Antennae 12 segmented (scape, pedicel and 10 flagellomeres) (Figs. 2B,5) with antennal length 7.44 ± 0.036 mm and the antennal scape is short, measuring 2.54 ± 0.08 mm (Table 1) in length and scape index is 90.58 (Table 2).

In lateral view, the dorsum of mesosoma pilosity is present. The shape is convex, with sharply distinct promesonotal suture, metanotal groove and mesonotum; pronotum has cavernous curved rugae. The mesosomal length is 4.05 ± 0.02 mm and weber's length is 4.17 ± 0.02 mm. In dorsal view, mesosoma is gradually narrowing from pronotum to propodeum; Pronotum has cavernous and regular transverse rugae; mesonotum and propodium have transverse rugae. The shoulders of the pronotum have a pair of blunt spines (Fig. 2D). The margin of the pronotum is convex. The posterodorsal corner of the propodeum is rounded, forming a blunt angle, with four large denticles (Figs. 2D,3D). The foreleg, midleg and hindleg contain comb-like tibial spur. The measurement of the length of forelegs, midlegs and hindlegs are 8.2 ± 0.04 mm, 8.31 ± 0.03 mm and 10.39 ± 0.07 mm respectively (Table 1).

In frontal view, the Petiolar node is concave apically, pilosity present and in lateral view narrowly triangular with straight anterior and posterior margins (Figs. 2E,3E). The subpetiolar process is smooth, trapezoidal, narrowed behind, with the anteroventral corner right-angled and the posteroventral corner more acute. The length of the petiolar node is 1.25 ± 0.06 mm. Gaster is smooth with 2.01 ± 0.03 mm length, pilosity and sting present (Figs. 2F,3F).



Fig. 1. Whole body of *Odontoponera denticulata* under stereozoom microscope. Scale bar = 2 mm.

Table 1
Various morphological measurements (Mean \pm SE) of *Odontoponera denticulata*.
 $n=6$.

SI No.	Different Body Parts	Measurements (mm)
1	Head Length (HL)	3.2 \pm 0.03
2	Head Width (HW)	2.81 \pm 0.02
3	Scape Length (SL)	2.54 \pm 0.08
4	Antennae Length (AL)	7.44 \pm 0.04
5	Pronotal Width (PrW)	1.7 \pm 0.01
6	Mesosomal Length (ML)	4.05 \pm 0.02
7	Weber's Length (WL)	4.17 \pm 0.02
8	Petiolar Length (PL)	1.25 \pm 0.06
9	Gaster Length (GL)	2.01 \pm 0.03
10	Foreleg Length (FLL)	8.2 \pm 0.04
11	Midleg Length (MLL)	8.31 \pm 0.03
12	Hindleg Length (HLL)	10.39 \pm 0.07
13	Total Length (TL)	10.35 \pm 0.05

3.2. Sequence analysis

DNA sequences from a portion of the COI region are analyzed from the present investigated ant species. The sequence is compared to eighteen different ant species having query cover 81–100%. Although, it shows 100% query cover with 3 ant species namely *Odontomachus cephalotes* (Accession: KU504882.1), *Anochetus paripungens* (Accession: KU504852.1) and *Monomorium cyaneum* (Accession: KT356485.1, KT356494.1, KT356533.1) but shows only 81.18%–83.78% identity with them. On the other hand, maximum identity (86.08%) was observed with *Odontoponera transversa* (Accession: KX664677.1) with 98% query cover (Table 3). The obtained COI sequence submitted to the NCBI-GenBank under the accession number MN 380424.

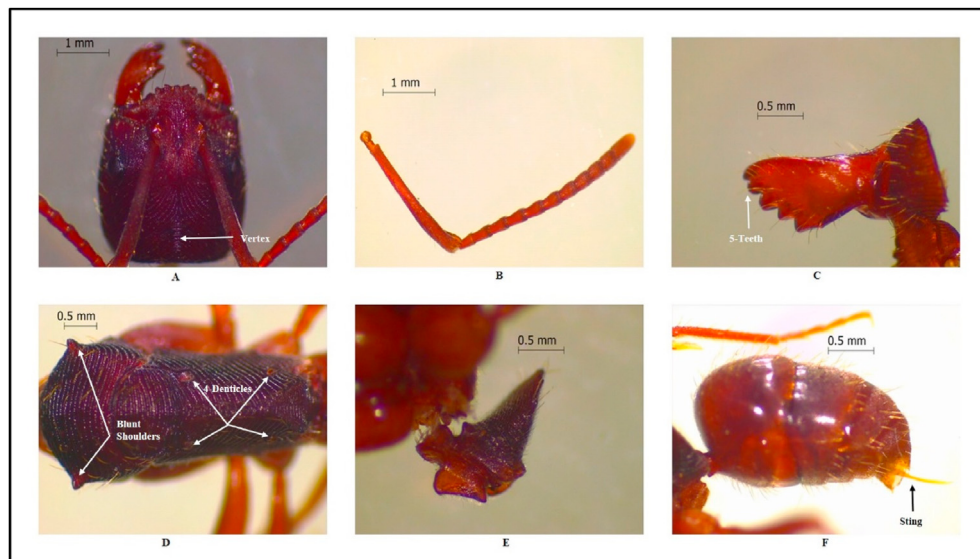


Fig. 2. Different body parts of *Odontoponera denticulata* under stereozoom microscope (A) Head in full face view showing vertex (B) 12-segmented Antennae (C) Mandibles showing 5-teeth (D) Dorsal view of Mesosoma showing 4-Denticles and Blunt Shoulders (E) Petiole (F) Gaster showing sting (20X). Scale bar = 1 mm (A,B), 0.5 mm (C,D,E,F).

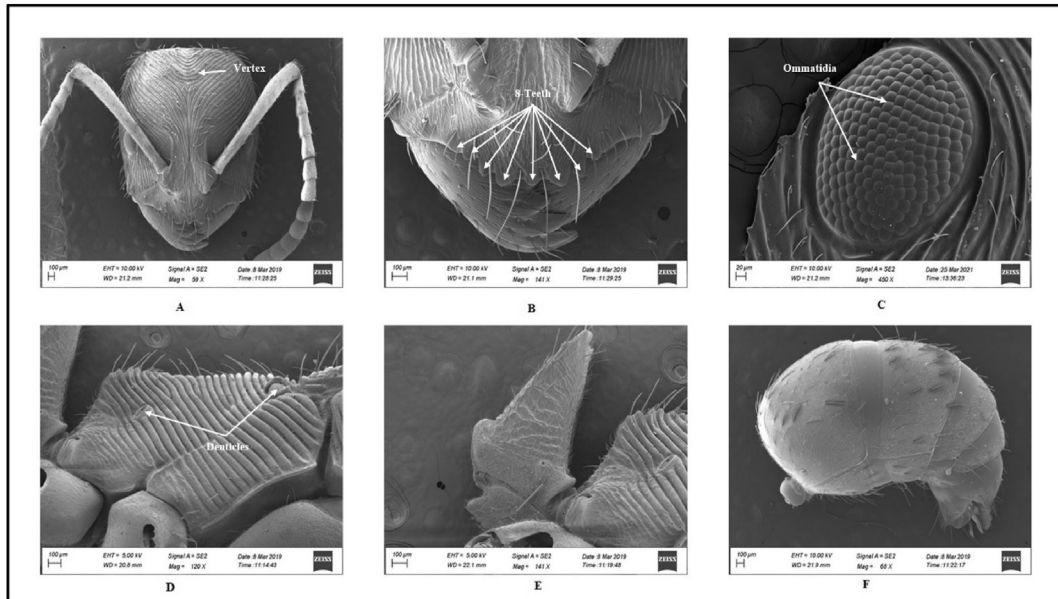


Fig. 3. SEM micrograph of different body parts of *Odontoponera denticulata* (A) Head showing less defined raised vertex (B) Clypeus showing 8-Teeth (C) Compound eyes showing ommatidia (D) Lateral view of mesosoma showing Denticles (E) Petiole (F) Gaster. Scale bar = 100 µm (A,B,D,E,F), 20 µm (C).

Table 2
Various morphological indices of *Odontoponera denticulata*.

SI No.	Morphological Indices	Values
1	Cephalic Index (CI)	87.71
2	Scape Index (SI)	90.58

3.3. Phylogenetic analysis

The phylogenetic tree reveals two main clades (Fig. 4). The first clade consists of two subclades representing the Myrmicinae subfamily (10 species). Similarly, the second clade consists of two subclades, where the first subclade representing the Dolichoderinae subfamily (1 species) and the second subclade representing the Ponerinae subfamily (8 species). In the second subclade, *O. denticulata* and *O. transversa* are branching from the same node, while the other 6 ant species belonging to the Ponerinae subfamily are branching from a different node (Fig. 4). The Kimura-2-Parameter distance matrix of individuals within species with minimum 0.003 and maximum 0.226 (Table 4).

3.4. Gross antennal morphology

Antennae of *O. denticulata* are geniculate type and consist of scape, pedicel, and 10 segmented flagellum (Fig. 5). Scape, the first antennal segment, measures approximately 2339.33 ± 47.39 µm in length and 156.03 ± 0.32 µm in width of median regions of worker ants (Table 5). Pedicel, the second and shortest segment of antenna measures approximately 334.23 ± 3.96 µm in length and 134.91 ± 0.26 µm width in worker ants (Table 5). Flagellum, the third and longest region of the antennae measures approximately 3316 ± 25.15 µm in length and 135.7 ± 0.58 µm in width at the median region of worker ants (Table 5).

3.4.1. Types and distribution of different antennal sensilla

Microscopic observations indicate that nine types of antennal sensilla are present in the antenna of *O. denticulata* including Böhm Bristles (BB1, BB2), sensilla Trichodea (ST1, ST2), Sensilla Chaetica

(SCh), Sensilla Basicornica (SB1, SB2), Sensilla Coeloconica (SCo) and Sensilla Campaniformia (SCa).

These sensilla types are classified based on the shape, size, presence or absence of pores on the surface, smooth or grooved surface and the position of sensilla i.e. inside the pit or on the surface of the cuticle. Their characteristic morphological features are summarized in Table 6.

Böhm Bristles 1 (BB1): BB1 are short, smooth surface, non-porous, straight hairs with a blunt tip and broad at the base measuring 6.83 ± 0.24 µm in length and 1.27 ± 0.05 µm in basal diameter (Table 6) (Fig. 6A and B). BB1 are found in the scape ball and the joints between scape and pedicel.

Böhm Bristles 2 (BB2): BB2 are cone-shaped hairs with smooth surfaces, non-porous and pointed tips (Fig. 6C and D). They measure 2.47 ± 0.03 µm in length and 0.93 ± 0.02 µm in basal diameter (Table 6). BB2 are observed in the intersegmental joints between flagellomeres.

Sensilla Trichodea 1 (ST1): ST1 are straight or slightly curved hairs with a blunt tip (Fig. 6E). Pores present at the surface of the sensilla (Fig. 6F). They measure 31.71 ± 4.12 µm in length and 1.89 ± 0.15 µm in basal diameter (Table 6). ST1 are abundantly distributed throughout the antennae.

Sensilla Trichodea 2 (ST2): ST2 are thick sword-shaped, blunt tip and straight hairs (Fig. 6G). Pores present throughout the surface wall (Fig. 6H). They measure 27.68 ± 0.82 µm in length and 3.43 ± 0.27 µm in basal diameter (Table 6). ST2 are found only in the flagellomeres.

Sensilla Basicornica 1 (SB1): SB1 are straight, long sensilla with a blunt and slightly depressed tip (Fig. 7A). Pores present throughout the surface wall (Fig. 7B). They have 22.96 ± 0.77 µm length and 3.5 ± 0.2 µm basal diameter (Table 6). SB1 are observed in the flagellomeres.

Sensilla Basicornica 2 (SB2): SB2 are straight, short, blunt tip and thumb-like hairs (Fig. 7C). Pores present throughout the surface wall (Fig. 7D). They have a mean length of 8.89 ± 0.62 µm and basal diameter of 2.1 ± 0.11 µm (Table 6). SB2 are also observed in the flagellomeres.

Sensilla Chaetica (SCh): SCh are long, blunt tips and straight hairs with longitudinal grooves present on the surface (Fig. 7E and

Table 3

Sequence analysis result based on BLAST.

Description	Max score	Total score	Query cover	E value	Ident	Accession
<i>Odontoponera transversa</i> voucher WQ001 cytochrome c oxidase subunit I (COI) gene, partial cds; mitochondrial	744	744	98%	0	86.08%	KX664677.1
<i>Odontomachus cephalotes</i> voucher CASENT0200850 cytochrome oxidase subunit I (COI) gene, partial cds; mitochondrial	688	688	100%	0	83.78	KU504882.1
<i>Odontomachus</i> sp. ODON017 voucher MIAN09-074 cytochrome oxidase subunit 1 (COI) gene, partial cds; mitochondrial	560	560	98%	4.00E-155	82.68	KU146044.1
<i>Aphaenogaster occidentalis</i> voucher UCDC PSW14381 CASENT0106090 cytochrome oxidase subunit 1 (COI) gene, partial cds; mitochondrial	547	547	98%	3.00E-151	82.45	JQ742634.1
<i>Pheidole laselva</i> voucher RA0185 cytochrome oxidase subunit I (coxl) gene, partial cds; mitochondrial	544	544	99%	4.00E-150	82.3	EF518361.1
<i>Tetramorium norvigi</i> voucher CASENT0059930-D01 cytochrome oxidase subunit 1 (COI) gene, partial cds; mitochondrial	536	536	98%	7.00E-148	82.19	HQ547326.1
<i>Anochetus paripungens</i> voucher USNMENT01124355 cytochrome oxidase subunit I (COI) gene, partial cds; mitochondrial	547	547	100%	3.00E-151	82.14	KU504852.1
<i>Syllophopsis sechellensis</i> voucher fossQM15141_58 cytochrome oxidase subunit I (COI) gene, partial cds; mitochondrial	521	521	95%	2.00E-143	82.14	KJ847482.1
<i>Technomyrmex albipes</i> voucher CASENT0191096-D01 cytochrome oxidase subunit 1 (COI) gene, partial cds; mitochondrial	531	531	98%	3.00E-146	81.97	HQ925258.1
<i>Pheidole</i> sp. JTL-110 voucher 10COSTA-0542 cytochrome oxidase subunit 1 (COI) gene, partial cds; mitochondrial	514	514	96%	3.00E-141	81.76	HQ545824.1
<i>Tetramorium scytalum</i> voucher CASENT0136855-D01 cytochrome oxidase subunit 1 (COI) gene, partial cds; mitochondrial	520	520	98%	7.00E-143	81.63	GU709661.1
<i>Tetramorium norvigi</i> voucher CASENT0497059-D01 cytochrome oxidase subunit 1 (COI) gene, partial cds; mitochondrial	514	514	98%	3.00E-141	81.62	HQ547454.1
<i>Pachycondyla</i> sp. JTL014 voucher BIOUG01264-C06 cytochrome oxidase subunit 1 (COI) gene, partial cds; mitochondrial	516	516	97%	1.00E-141	81.56	KF371366.1
<i>Monomorium cyaneum</i> isolate MJF226Q1 cytochrome oxidase subunit I (COI) gene, partial cds; mitochondrial	525	525	100%	2.00E-144	81.49	KT356485.1
<i>Tetramorium delagoense</i> voucher CASENT0052371-D01 cytochrome oxidase subunit 1 (COI) gene, partial cds; mitochondrial	512	512	98%	1.00E-140	81.48	HQ546816.1
<i>Pheidole longispinosa</i> voucher CASENT0061669-D01 cytochrome oxidase subunit 1 (COI) gene, partial cds; mitochondrial	514	514	98%	3.00E-141	81.48	HM880865.1
<i>Ponerinae</i> sp. BOLD:AAB9409 voucher BIOUG01158-H06 cytochrome oxidase subunit 1 (COI) gene, partial cds; mitochondrial	510	510	97%	4.00E-140	81.4	KF371402.1
<i>Pachycondyla</i> sp. JTL014 voucher BIOUG01264-D05 cytochrome oxidase subunit 1 (COI) gene, partial cds; mitochondrial	510	510	97%	4.00E-140	81.4	KF371375.1
<i>Monomorium cyaneum</i> isolate MJF285 cytochrome oxidase subunit I (COI) gene, partial cds; mitochondrial	520	520	100%	7.00E-143	81.37	KT356494.1
<i>Messor capensis</i> voucher AFR-PGH2009.09.06-wp37-01 cytochrome oxidase subunit 1 (COI) gene, partial cds; mitochondrial	512	512	98%	1.00E-140	81.29	JN283629.1
<i>Monomorium cyaneum</i> isolate RAJ3541Q1 cytochrome oxidase subunit I (COI) gene, partial cds; mitochondrial	514	514	100%	3.00E-141	81.18	KT356533.1

F). Pores present at the tip (**Fig. 7G**). They have a mean length of $100.98 \pm 13.65 \mu\text{m}$ and basal diameter of $4.93 \pm 0.63 \mu\text{m}$ (**Table 6**). SCh are present throughout the antennae.

Sensilla Campaniformia (SCa): SCa are seen as domed structures with a central cavity. They have a diameter of $7.56 \pm 0.26 \mu\text{m}$ (**Fig. 7H**). SCa are present in the flagellomeres.

Sensilla Coeloconica (SCo): SCo appeared as a small opening at the cuticle (**Fig. 8A**). The opening of SCo measures $2.25 \pm 0.17 \mu\text{m}$ in diameter (**Table 6**). In high magnification under SEM, a peg in the pit was observed (**Fig. 8B**). SCo are present in the flagellomeres.

4. Discussion

In the present study using both morphological and molecular approaches, the species is confirmed as *Odontoponera denticulata*. The specimen possesses a pronotum with a pair of laterally directed triangular teeth, mandibles with 5 teeth and the clypeal margin with 8 blunt teeth which are characters of the genus *Odontoponera* as described by Bolton (1994). Furthermore, it also acquires 12-segmented antennae, vertex on the head with a less defined raised area, propodeum with large four denticles, which are the identification key to the species *Odontoponera denticulata* as documented by Yamane (2009). The same study also mentioned taxonomical

description of its close species, *Odontoponera transversa* which bears vertex of the head with well-developed raised area and propodeum with only two denticles as their identification key. In the present study, the investigated species was found foraging on the ground and mostly preferred human-disturbed areas which is found quite similar with the findings of Yamane (2009). In addition to this, morphometric analysis of different body parts of the investigated species is done. The result revealed that the whole-body length of the worker caste of the investigated species is in the range of 10–11 mm, head length 2.5–3.5 mm, mesosomal length 3.5–4.5 mm, gaster length 2–3 mm. From the morphometric analysis, it is also confirmed that the forelegs are the shortest ($8.19 \pm 0.04 \text{ mm}$) and hindlegs are the longest ($10.39 \pm 0.06 \text{ mm}$) pair of legs present in the species. The morphometric measurements recorded in the present investigation are almost similar to those reported by Wachkoo et al. (2020) but larger than those reported by Leong et al. (2017). This may be due to the different geographical areas and climatic conditions.

The COI barcode analysis of the present study shows the highest similarity (86.08%) of the sample to *Odontoponera transversa* as compared to the other seventeen species where percent similarity ranges from 81.18% to 83.78%. Based on the distance-based criteria (Meier et al. 2006), in which a query sequence are assigned to a

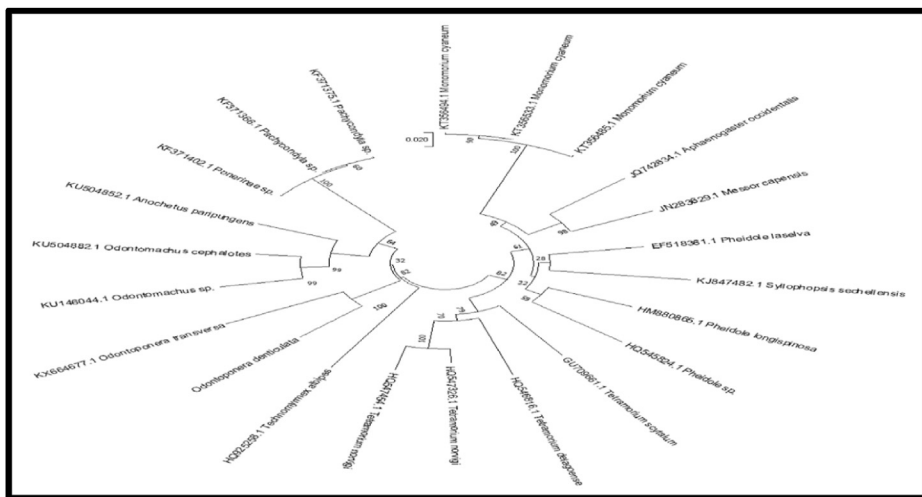


Fig. 4. Phylogenetic relationships of taxa based on COI sequences.

Table 4
Estimates of divergence between sequences.

Odontoponera denticulata									
KX664677.1	.155								
<i>Odontoponera transversa</i>									
KU146044.1	.200	.226							
<i>Odontomachus</i> sp.									
KU504882.1	.183	.211	.096						
<i>Odontomachus cephalotes</i>									
KU504852.1	.208	.233	.147	.108					
<i>Anochetus paripungens</i>									
JQ742634.1	.209	.262	.231	.235	.240				
<i>Aphaenogaster occidentalis</i>									
EF518361.1	.214	.255	.248	.200	.208	.190			
<i>Pheidole laselva</i>									
HQ547326.1	.211	.238	.189	.163	.182	.187	.189		
<i>Tetramorium norvigi</i>									
HQ925258.1	.220	.250	.240	.233	.236	.255	.216	.200	
<i>Technomyrmex albipes</i>									
KT356485.1	.218	.249	.223	.190	.209	.191	.182	.191	.255
<i>Monomorium cyaneum</i>									
KJ847482.1	.210	.239	.254	.220	.212	.212	.168	.190	.248
<i>Syllophopsis sechellensis</i>									.223
KT356494.1	.222	.258	.223	.195	.212	.191	.189	.193	.262
<i>Monomorium cyaneum</i>									.009
GU709661.1	.221	.236	.229	.198	.201	.197	.194	.133	.230
<i>Tetramorium scytalum</i>									.211
KF371366.1	.217	.226	.181	.174	.176	.236	.234	.175	.204
<i>Pachycondyla</i> sp.									.227
KT356533.1	.222	.258	.223	.194	.211	.191	.186	.193	.260
<i>Monomorium cyaneum</i>									.006
HM880865.1	.217	.246	.240	.186	.219	.186	.137	.179	.223
<i>Pheidole longispinosa</i>									.174
HQ545824.1	.215	.266	.248	.247	.235	.187	.170	.202	.237
<i>Pheidole</i> sp.									.196
HQ547454.1	.221	.238	.209	.182	.193	.203	.201	.054	.214
<i>Tetramorium norvigi</i>									.209
JN283629.1	.218	.251	.232	.205	.200	.136	.165	.180	.222
<i>Messor capensis</i>									.186
HQ546816.1	.224	.250	.247	.215	.211	.212	.210	.144	.230
<i>Tetramorium delagoense</i>									.215
KF371402.1	.219	.228	.181	.174	.176	.236	.234	.176	.202
<i>Ponerinae</i> sp.									.229
KF371375.1	.220	.229	.184	.176	.178	.237	.237	.176	.207
<i>Pachycondyla</i> sp.									.230
									.243
									.235
									.215
									.201
									.193
									.242
									.218
									.003

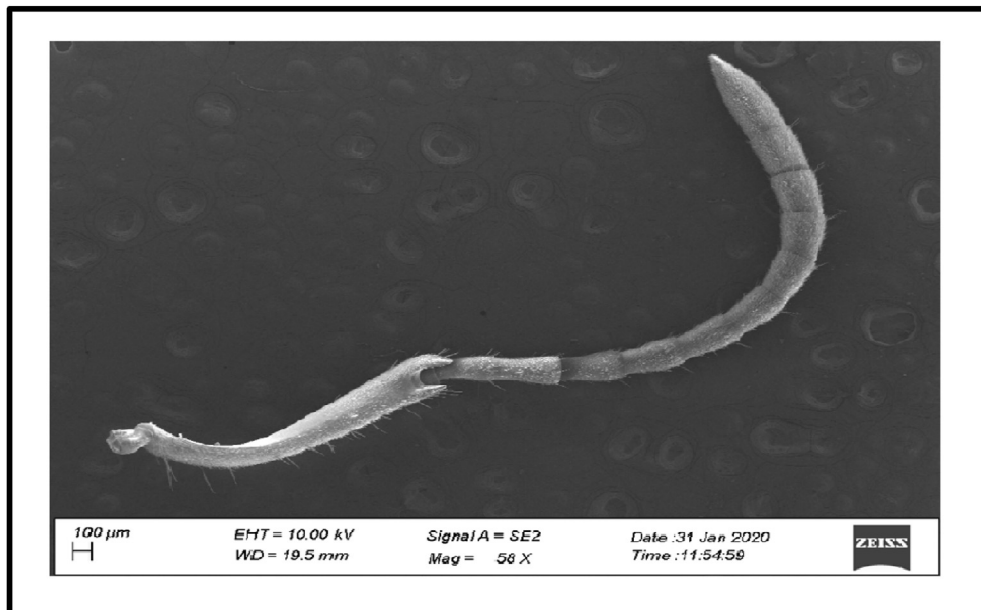


Fig. 5. SEM micrograph of *Odontoponera denticulata* antenna. Scale bar = 100 μm .

Table 5

Length and width (Mean \pm SE) of antennae segments of *Odontoponera denticulata*. $n=6$.

Antennal Segment	Length (μm)	Width (μm)
Scape	2339.33 \pm 47.39	156.03 \pm 0.32
Pedicel	334.23 \pm 3.96	134.91 \pm 0.26
Flagellum	3316 \pm 25.15	135.7 \pm 0.58

species of the best-matched barcode where the similarity between the query and the best-matched barcode is less than 95% for all intraspecific distances; it is confirmed that the investigated species is not *Odontoponera transversa*. Similar work was done by Ng'endo et al. (2013), where DNA barcoding was used to species-level identification of hyperdiverse ant genus *Pheidole* to test if the morphology-based assignment of individuals into species is supported by DNA-based species delimitation. Also, in the detailed taxonomy of armadillo ants genus *Tatuidris*, both morphological and molecular taxonomy was used (Donoso 2012).

The phylogenetic tree also revealed that the present investigated ant species is close relative to *Odontoponera transversa*. But from the morphological approach, it is confirmed that the species is *Odontoponera denticulata*.

In addition to this, the present investigation also reveals that nine different types of antennal sensilla are widely distributed on the surface of the antennae. The abundance of antennal sensilla is gradually increasing from the first segment (scape) to the last segment (10th segment of flagellum) of the antennae (Table 7).

BB1 are found in the scape ball, joints between the scape and pedicel of the antennae. These sensilla correspond to the Böhm Bristles present in other insects including bruchid beetles (Hu et al. 2009), lepidopteran *Automeris liberia* (da Silva et al. 2019), *Erannis ankeraria* (Liu et al. 2019), longhorn beetle *Glenea cantor* (Dong et al. 2020), *Earias vittella* (Rani et al. 2021) and thrips (Liu et al. 2021). On the other hand, BB2 are observed in the intersegmental joints between the flagellomere segments. These sensilla correspond to the "Sensilla basiconica subtype 3" of Carabid beetle (Giglio et al. 2008). This finding was in contrast with the findings of previous workers as they reported that böhm bristles are found only in the scape and pedicel but not in the flagellum (Crook et al. 2008; Giulio et al. 2012; Ma & Du 2000; Yang et al. 2009). Böhm Bristles act as a mechanoreceptor and monitor the position of the antennae and their movements which occur due to the activity of the antenna muscles in response to sensory stimulus (Schneider 1964; Krishnan et al. 2012).

Table 6

Morphological types of antennal sensilla in *Odontoponera denticulata* ($n = 12$).

Types of sensilla	Morphological characteristics of sensilla					
	Length (Mean \pm SE) (μm)	Diameter (Mean \pm SE) (μm)	Tip	Wall	Shape	Pores
BB1	6.83 \pm 0.24	1.27 \pm 0.05	Blunt	Smooth	Straight	Absent
BB2	2.47 \pm 0.03	0.93 \pm 0.02	Blunt	Smooth	Straight	Absent
ST1	31.71 \pm 4.12	1.89 \pm 0.15	Smooth	Straight/Curved	Present	
ST2	27.68 \pm 0.82	3.43 \pm 0.27	Blunt	Smooth	Straight/Curved	Present
SB1	22.96 \pm 0.77	3.5 \pm 0.2	Blunt	Smooth	Straight	Present
SB2	8.89 \pm 0.62	2.1 \pm 0.11	Blunt	Smooth	Straight	Present
SCh	100.98 \pm 13.65	4.93 \pm 0.63	Blunt	Grooved	Straight	Present
SCa	—	7.56 \pm 0.26	—	—	Dome shaped	Present
SCo	—	2.25 \pm 0.17	—	—	—	—

BB1: Böhm Bristles 1; BB2: Böhm Bristles 2; ST1: Sensilla Trichodea 1; ST2: Sensilla Trichodea 2; SB1: Sensilla Basiconica 1; SB2: Sensilla Basiconica 2; SCh: Sensilla Chaetica; SCa: Sensilla Campaniformia; SCo: Sensilla Coeloconica.

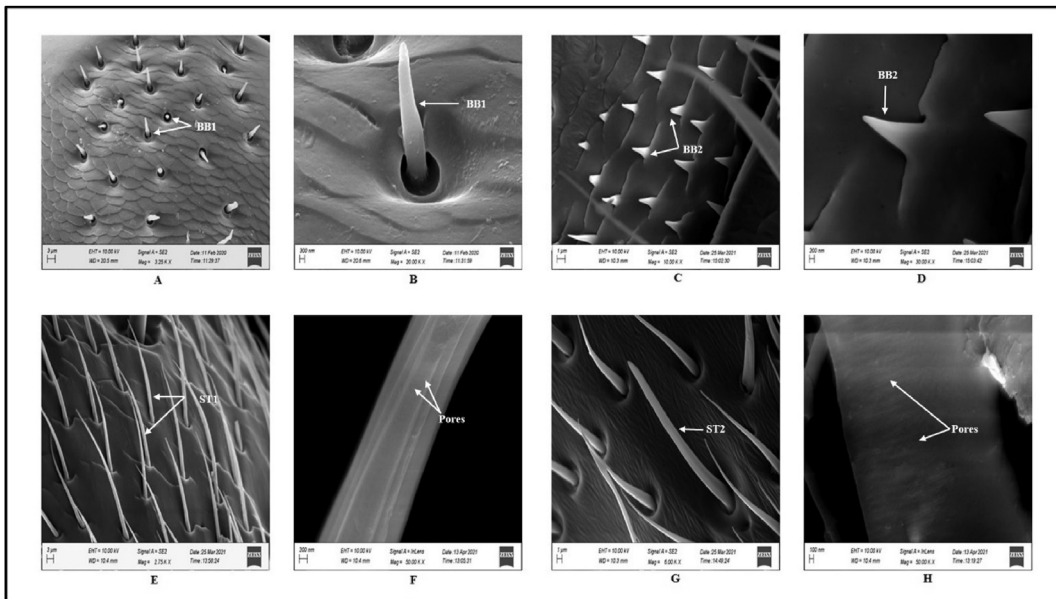


Fig. 6. SEM micrograph of antennal sensilla of *Odontoponera denticulata* (A) Böhm Bristles 1 (BB1) present in joints between scape and pedicel (B) Böhm Bristles 1 (BB1) in higher magnification (C) Böhm Bristles 2 (BB2) present between flagellomeres (D) Böhm Bristles 2 (BB2) in higher magnification (E) Sensilla Trichodea 1 (ST1) (F) Surface wall of Sensilla Trichodea 1 (ST1) showing pores (G) Sensilla Trichodea 2 (ST2) (H) Surface wall of Sensilla Trichodea 2 (ST2) showing pores. Scale bar = 3 µm (A,E), 300 nm (B), 1 µm (C,G), 200 nm (D,F), 100 nm (H).

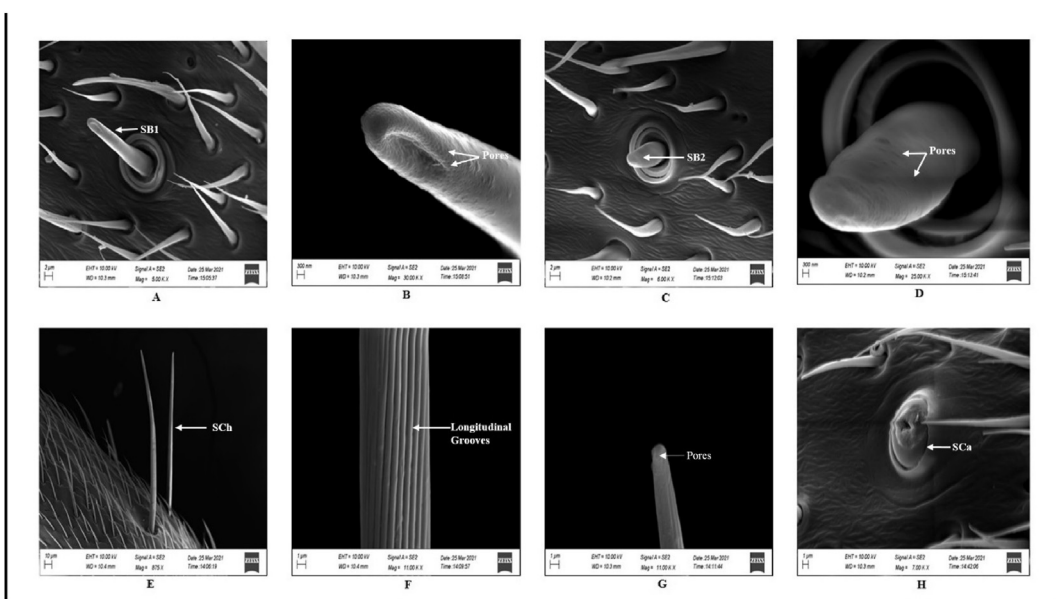


Fig. 7. SEM micrograph of antennal sensilla of *Odontoponera denticulata* (A) Flagellomere showing SB1 (Sensilla Basiconica 1) (B) Surface wall of Sensilla Basiconica 1 (SB1) showing pores (C) Flagellomere showing Sensilla Basiconica 2 (SB2) (D) Surface wall of Sensilla Basiconica 1 (SB1) showing pores (E) Flagellomeres showing Sensilla Chaetica (SCh) (F) Surface wall of Sensilla Chaetica (SCh) showing longitudinal grooves (G) Tip of Sensilla Chaetica (SCh) showing pores (H) Flagellomeres showing Sensilla Campaniformia (SCa). Scale bar = 2 µm (A,C); 300 nm (B,D), 10 µm (E), 1 µm (F, G, H).

Sensilla Trichodea 1 (ST1) are the most abundant sensilla present in the antennae of *O. denticulata*. The external morphology of ST1 found in the present study is similar to the “trichoid II sensillum” of *Camponotus japonicus* (Nakanishi et al. 2009). Their porous surface wall suggests that they act as an olfactory receptor (Nakanishi et al. 2009). These sensilla may help to locate food sources as well as recognize colony members (Zacharuk 1985; Shanbhag et al. 1995). ST2 are distributed only in the flagellomere region and morphologically similar to the “Trichoid-I” sensillum of

Camponotus japonicus (Nakanishi et al., 2009) and “Trichoid Curvata sensillum” of previously reported ant species (Dumpert 1972b; Hashimoto 1990; Renthal et al. 2003). Their porous surface wall indicates that they act as olfactory receptors and respond to the volatile odours and pheromones (Renthal et al. 2003). Electrophysiological analysis in ants has revealed that this type of sensilla respond quickly to stimulation with alarm substances (Dumpert 1972a) and diverse organic compounds including pheromones (Dumpert 1972b).

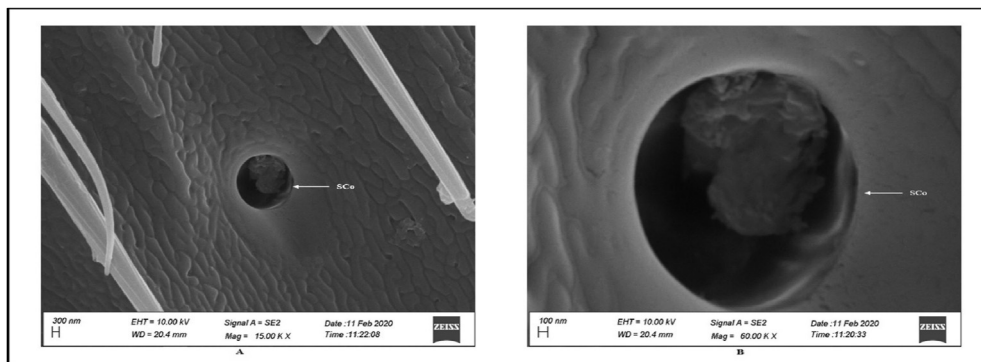


Fig. 8. SEM micrograph of different antennal sensilla found in *Odontoponera denticulata* (A) Surface of the flagellomere showing SCo (Sensilla Coeloconica) (B) SCo (Sensilla Coeloconica) in higher magnification. Scale bar = 300 nm (A), 100 nm (B).

Sensilla Basiconica 1 observed in the present investigation corresponds to the sensilla basiconica of other ant species (Hashimoto et al. 1990). The external morphology of SB2 are similar to the “basiconic sensillum” of Carpenter ant *Camponotus compressus* (Nakanishi et al. 2009; Ozaki et al. 2005) and fire ants *Solenopsis invicta* (Renthal et al. 2003). It is already reported that sensilla basiconica are female-specific and completely absent in the male caste of ants (Renthal et al. 2003; Nakanishi et al. 2009) and honey bees (Esslen & Kaissling 1976; Nishino et al. 2009). The porous surface wall of sensilla basiconica indicates that they act as olfactory receptors (Altner & Prillinger 1980; Keil 1999). Previous researchers suggested that sensilla basiconica may be CO₂-sensitive (Shanbhag et al. 1999) and acts as both contact and volatile chemoreceptors (Renthal et al. 2003; Ozaki et al. 2005). With the help of this sensilla, ants can recognize the nestmate and non-nestmate discrimination (Ozaki et al. 2005). Electrophysiological analysis in *Camponotus floridanus* has revealed that Sensilla Basiconica contains multiple olfactory receptor neurons which are differentially sensitive to cuticular hydrocarbons from nestmates and non-nestmates (Sharma et al. 2015).

Sensilla Chaetica are the longest sensilla distributed throughout the antennae of *O. denticulata*. The external morphology of Sensilla Chaetica was similar to the previously reported other ant species (Dumpert 1972b; Hashimoto 1990; Nakanishi et al. 2009). The presence of pores at the tip and the absence of pores on the longitudinal grooves of the surface wall suggested that they may act as contact chemoreceptors (Altner & Prillinger 1980).

Sensilla Campaniformia observed in the present investigation are morphologically similar to the Campaniform sensilla of

Odontomachus (Ehmer & Gronenberg 1997). It is an established fact that these sensilla are situated in the areas of cuticular surfaces that are subject to stress (Ahmad et al. 2016). In the present investigation, these sensilla are recorded in all flagellomere segments. This was in conformity with that of Marques-Silva et al. (2006), who reported that campaniform sensilla are located at the apex of the antennomere of *Dinoponera lucida*. In contrast, these sensilla are reported exclusively at the pedicel of antennae (Schneider 1964) and both scape and pedicel of antennae of *Odontomachus* (Ehmer & Gronenberg 1997). These sensilla act as mechanoreceptors and help in monitoring cuticular stress or any other mechanical deformations (Catalá 1997).

Sensilla coeloconica are distributed mainly in the 8th, 9th and 10th flagellomere segments. Previous workers reported that as compared to the other sensilla, sensilla coeloconica are found in low numbers on the antennae of ants as well as other insects (Dumpert 1972b; Tominaga & Yokohari 1982; Itoh et al. 1984; Nishikawa et al. 1985; Hashimoto 1990; Iwasaki et al. 1995; Renthal et al. 2003). The diameter of the external opening of SCo in the present investigation is similar to the external opening of SCo of the Formicidae family (Hashimoto 1990). In red imported fire ants *Solenopsis invicta*, coeloconic sensilla are described to have chemoreceptors in function (Renthal et al. 2003). But, electrophysiology and ultrastructural study of leaf-cutting ants *Atta vollenweideri* has shown that they are thermosensitive (Ruchty et al. 2009). It was reported that with the help of these sensilla, workers of social insects can detect the most appropriate weather conditions for foraging (Kleineidam & Tautz 1996).

Table 7

Abundance of Antennal sensilla in a defined area (10000 µm²) of various antennae segments. n = 6.

Antennae segments		Total number of Sensilla (Mean ± SE)
Scape	Basal	16 ± 0.58
	Median	18.33 ± 0.88
	Proximal	18.167 ± 0.79
Pedicel		28.833 ± 2.25
1st Flagellomere		30.67 ± 1.35
2nd Flagellomere		35.83 ± 1.08
3rd Flagellomere		38 ± 1.23
4th Flagellomere		41.67 ± 0.76
5th Flagellomere		45.83 ± 0.94
6th Flagellomere		48.83 ± 0.95
7th Flagellomere		56 ± 1.15
8th Flagellomere		69.16 ± 1.24
9th Flagellomere		74.83 ± 1.67
10th Flagellomere		83.5 ± 1.83

5. Conclusion

From the study, it can be concluded that both the morphological and molecular approaches are helpful for the identification of ant species. Since Yamane (2009) differentiates *Odontoponera denticulata* and *Odontoponera transversa* based on their morphological characters but the present investigation suggests that these two species are also genetically different from each other and this information would be helpful for further study of this ant species. In addition to this, we have also done identification and characterization of nine different antennal sensilla found in *Odontoponera denticulata* by using SEM. The probable function of each type of sensillum is speculated through comparison with other previous investigations.

Declaration of competing interest

The authors declare that they have no known competing financial interests or personal relationships that could have appeared to influence the work reported in this paper.

Acknowledgements

This work was supported by the Department of Biotechnology, Government of India (Project No. DBT/In/Indo-US/Foldscope/39/2015). The authors are grateful to the Head of the Department of Zoology for his support. Authors acknowledge Central Instruments Facility (CIF) & BIF Facility of Gauhati University. The authors are also thankful to Genombio, Bangalore for offering service in the sequencing of the gene.

References

- Ahmad, A., Parveen, S., Brozek, J., Dey, D., 2016. Antennal sensilla of phytophagous and predatory pentatomids (Hemiptera: pentatomidae): a comparative study of four genera. *Zool. Anz.* 261, 48–55.
- Altner, H., Prillinger, L., 1980. Ultrastructure of invertebrate chemo- thermo-, and hygroreceptors and its functional significance. *Int. Rev. Cytol.* 67, 69–139.
- Babu, M.J., Ankolekar, S.M., Rajashekhar, K.P., 2011. Castes of the weaver ant *Oecophylla smaragdina* (Fabricius) differ in the organization of sensilla on their antennae and mouthparts. *Curr. Sci.* 101 (6), 755–764.
- Bharti, H., 2008. Altitudinal diversity of ants in himalayan regions (Hymenoptera: Formicidae). *Sociobiology* 52, 305–322.
- Bharti, H., 2011. List of Indian ants (Hymenoptera: Formicidae). *Halteres* 3, 79–87.
- Bharti, H., Sharma, Y.P., Bharti, M., Pfeiffer, M., 2013. Ant species richness, endemism and functional groups, along an elevational gradient in the Himalayas. *Asian Myrmecology* 5, 79–101.
- Bharti, H., Bharti, M., Pfeiffer, M., 2016. Ants as bioindicators of ecosystem health in Shivalik Mountains of Himalayas: assessment of species diversity and invasive species. *Asian Myrmecology* 8, 1–15.
- Bolton, B., 1994. Identification Guide to the Ant Genera of World. Harvard University Press, Cambridge.
- Bolton, B., 1995. A New General Catalogue of the Ants of the World. Harvard University Press, Cambridge.
- Catalá, S.S., 1997. Antennal sensilla of triatominae (Hemiptera, reduviidae): a comparative study of five genera. *Int. J. Insect Morphol. Embryol.* 26 (2), 67–13.
- Chapman, R.F., 1998. The Insects: Structure and Function, fourth ed. Cambridge University Press, United Kingdom.
- Creighton, W.S., 1929. New forms of *Odontoponera transversa*. *Psyche* 36, 150–154.
- Crook, D.J., Kerri, L.M., Mastro, V.C., 2008. Sensilla on the antennal flagellum of *Sirex noctilio* (Hymenoptera: siricidae). *Ann. Entomol. Soc. Am.* 101 (6), 1094–1102.
- da Silva, K.B., da Silva, C.B., Júnior, K.A., de Freitas, J.M., de Freitas, J.D., Chia, G.S., Tinoco, R.S., da Costa, J.G., Goulart, H.F., Santana, A.E., 2019. Morphology and distribution of antennal sensilla of *Automeris liberia* (Lepidoptera: saturniidae). *Micron* 123, 102682.
- Dalla Torre de, C.G., 1893. CatalogusHymenopterum, hucusFuedescriptorum systematicus et synonymicus. Lipsiae.
- De Facci, M., Wallén, R., Hallberg, E., Anderbrant, O., 2011. Flagellar sensilla of the eusocial gall-inducing thrips *Kladothrips intermedius* and its kleptoparasite, *Koptothrips dyskratus* (Thysanoptera: phlaeothripinae). *Arthropod Struct. Dev.* 40 (6), 495–508.
- Dong, Z., Yang, Y., Dou, F., Zhang, Y., Huang, H., Zheng, X., Wang, X., Lu, W., 2020. Observations on the ultrastructure of antennal sensilla of adult *Glenea cantor* (cerambycidae: lamiinae). *J. Insect Sci.* 20 (2), 7.
- Donoso, D.A., 2012. Additions to the taxonomy of the armadillo ants (Hymenoptera, Formicidae, Tatuidris). *Zootaxa* 3503, 61–81.
- Dumpert, K., 1972a. Alarmstoffrezeptoren auf der Antenne von *Lasius fuliginosus* (Latr.) (Hymenoptera, Formicidae). *Z. Vergl. Physiol.* 76, 403–425.
- Dumpert, K., 1972b. Bau und Verteilung der Sensillen auf der Antennengeissel von *Lasius fuliginosus* (Latr.) (Hymenoptera, Formicidae). *Z. Morphol. Tiere* 73, 95–116.
- EHmer, B., Gronenberg, W., 1997. Proprioceptors and fast antennal reflexes in the ant *Odontomachus* (Formicidae, Ponerinae). *Cell Tissue Res.* 290, 153–165.
- Esslen, J., Kaissling, K.E., 1976. Zahl und Verteilung antennaler Sensillen bei der Honigbiene (*Apis mellifera* L.). *Zoomorphologie* 83 (3), 227–251.
- Felsenstein, J., 1985. Confidence limits on phylogenies: an approach using the bootstrap. *Evolution* 39 (4), 783–791.
- Folmer, O., Black, M., Hoeh, W., Lutz, R., Vrijenhoek, R., 1994. DNA primers for amplification of mitochondrial cytochrome c oxidase subunit I from diverse metazoan invertebrates. *Mol. Mar. Biol. Biotechnol.* 3, 294–299.
- Gigliò, A., Brandmayr, P., Ferrero, E., Perrotta, E., Romeo, M., Zetto, T., Talarico, F., 2008. Comparative Antennal Morphometry and Sensilla Distribution Pattern of Three Species of Siagoninae (Coleoptera, Carabidae). *Back to Roots Back to Futur*. Sofia Moscow Pensoft, pp. 143–158.
- Giulio, A.D., Maurizi, E., Stacconi, M.V.R., Romani, R., 2012. Functional structure of antennal sensilla in the myrmecophilous beetle *Paussus favieri* (Coleoptera, Carabidae, Paussini). *Micron* 43, 705–719.
- Hajibabaei, M., Janzen, D.H., Burns, J.M., Hallwachs, W., Hebert, P.D.N., 2006. DNA barcodes distinguish species of tropical Lepidoptera. *Proceedings of the National Academy of Sciences USA* 103 (4), 968–971.
- Hashimoto, Y., 1990. Unique features of sensilla on the antennae of Formicidae (Hymenoptera). *Appl. Entomol. Zool* 25, 491–501.
- Hebert, P.D.N., Cywinski, A., Ball, S.L., DeWaard, J.R., 2003a. Biological identifications through DNA barcodes. *Proc. Roy. Soc. Lond. B Biol. Sci.* 270, 313–321.
- Hebert, P.D.N., Ratnasingham, S., DeWaard, J.R., 2003b. Barcoding animal life: cytochrome c oxidase subunit I divergences among closely related species. *Proc. Roy. Soc. Lond. B Biol. Sci.* 270, S96–S99.
- Hebert, P.D.N., Penton, E.H., Burns, J.M., Janzen, D.H., Hallwachs, W., 2004. Ten species in one: DNA barcoding reveals cryptic species in the neotropical skipper butterfly *Astraptesfulgorifer*. *Proceedings of Naional Academy of Sciences of the USA* 101 (41), 14812–14817.
- Hlaing, T., Tun-Lin, W., Somboon, P., Socheat, D., Setha, T., Min, S., Chang, M.S., Walton, C., 2009. Mitochondrial pseudogenes in the nuclear genome of *Aedes aegypti* mosquitoes: implications for past and future population genetic studies. *BMC Genet.* 10 (11), 1–12.
- Holldobler, B., Wilson, E.O., 1990. The Ants. Harvard University Press, Cambridge.
- Hu, F., Zhang, G.N., Wang, J.J., 2009. Scanning electron microscopy studies of antennal bruchid beetles, *Callosobruchus chinensis* (L.) and *Callosobruchus maculatus* (F.) (Coleoptera: bruchidae). *Micron* 40, 320–326.
- Itoh, T., Yokohari, F., Tominaga, Y., 1984. 2 types of antennal hygroreceptive and thermoreceptive sensilla of the cricket, *Gryllus bimaculatus* (De Geer). *Zool. Sci.* 1, 533–543.
- Iwasaki, M., Itoh, T., Yokohari, F., Tominaga, Y., 1995. Identification of antennal hygroreceptive sensillum and other sensilla of the firefly, *Luciola cruciata*. *Zool. Sci.* 12, 725–732.
- Jarman, S.N., Elliott, N.G., 2000. DNA evidence for morphological and cryptic Cenozoic speciations in the Anaspidae, 'living fossils' from the Triassic. *J. Evol. Biol.* 13, 624–633.
- Keil, T.A., 1999. Morphology and development of the peripheral olfactory organs. In: Hansson, B.S. (Ed.), Insect Olfaction. Springer, Heidelberg, pp. 5–47.
- Kleineidam, C., Tautz, J., 1996. Perception of carbon dioxide and other "air-conditioning" parameters in the leaf cutting ant *Atta cephalotes*. *Naturwissenschaften* 83 (12), 566–568.
- Kimura, M., 1980. A simple method for estimating evolutionary rates of base substitutions through comparative studies of nucleotide sequences. *J. Mol. Evol.* 16, 111–120.
- Knowlton, N., 1993. Sibling species in the sea. *Annu. Rev. Ecol. Systemat.* 24, 189–216.
- Krishnan, A., Prabhakar, S., Sudarsan, S., Sane, S.P., 2012. The neural mechanisms of antennal positioning in flying moths. *J. Exp. Biol.* 215 (17), 3096–3105.
- Kumar, N.P., Srinivasan, R., Jambulingam, P., 2012. DNA barcoding for identification of sand flies (Diptera: psychodidae) in India. *Molecular Ecology Resources* 12, 414–420.
- Leong, C., Shiao, S., Liu, J., Lin, C., Yamane, S., 2017. Records of *Odontoponera denticulata* (F. Smith, 1858) (Hymenoptera: Formicidae) from taiwan, with a note on sculptural variation in workers. *Jpn. J. Syst. Entomol.* 23 (1), 21–27.
- Liu, F., Li, F., Zhang, S., Kong, X., Zhang, Z., 2019. Ultrastructure of antennal sensilla of *Eranis ankeraria staudingeri* (Lepidoptera: geometridae). *Microsc. Res. Tech.* 82 (11), 1903–1910.
- Liu, Y.Q., Li, J., Ban, L.P., 2021. Morphology and distribution of antennal sensilla in three species of thripidae (thysanoptera) infesting alfalfa medicago sativa. *Insects* 12 (1), 81.
- Ma, R.Y., Du, J.W., 2000. Insect sensilla. *Entomol. Knowl.* 37 (3), 179–183.
- Marques-Silva, S., Matiello-Guss, C.P., Delabie, J.H., Mariano, C.S., Zanuncio, J.E., Serrão, J.E., 2006. Sensilla and secretory glands in the antennae of a primitive ant: *Dinoponera lucida* (Formicidae: Ponerinae). *Microsc. Res. Tech.* 69 (11), 885–890.

- Meier, R., Shiyang, K., Vaidya, G., Ng, P.K.L., 2006. DNA barcoding and taxonomy in Diptera: a tale of high intraspecific variability and low identification success. *Syst. Biol.* 55 (5), 715–728.
- Monaghan, M., Balke, M., Gregory, T., Vogler, A., 2005. DNA-based species delineation in tropical beetles using mitochondrial and nuclear markers. *Philos. Trans. R. Soc. Lond. B Biol. Sci.* 360 (1462), 1925–1933.
- Nakanishi, A., Nishino, H., Watanabe, H., Yokohari, F., Nishikawa, M., 2009. Sex-specific antennal sensory system in the ant *Camponotus japonicus*: structure and distribution of sensilla on the flagellum. *Cell Tissue Res.* 338, 79–97.
- Nation, J.L., 2002. Insect Physiology and Biochemistry. CRC Press, Boca Raton, FL, USA.
- Nishikawa, M., Yokohari, F., Ishibashi, T., 1985. The antennal thermoreceptor of the camel cricket, *Tachycines asynamorus*. *J. Insect Physiol.* 31, 517–524.
- Nishino, H., Nishikawa, M., Mizunami, M., Yokohari, F., 2009. Functional and topographic segregation of glomeruli revealed by local staining of antennal sensory neurons in the honeybee *Apis mellifera*. *J. Comp. Neurol.* 515, 161–180.
- Ng'endo, R.N., Osiemo, Z.B., Brandl, R., 2013. DNA barcodes for species identification in the hyperdiverse ant genus *Pheidole* (Formicidae: Myrmicinae). *J. Insect Sci.* 13 (27), 1–13.
- Ozaki, M., Wada-Yasumata, A., Fujikawa, K., Iwasaki, M., Yokohari, F., Satoji, Y., Nisimura, T., Yamaoka, R., 2005. Ant nesmate and non-nestmate discrimination by a chemosensory sensillum. *Science* 309, 311–314.
- Padial, J.M., Miralles, A., De La Riva, I., Vences, M., 2010. The integrative future of taxonomy. *Front. Zool.* 7, 1–16.
- Rani, A.T., Shashank, P.R., Meshram, N.M., Sagar, D., Srivastava, C., Pandey, K.K., Singh, J., 2021. Morphological characterization of antennal sensilla of *Earias vittella* (Fabricius) (Lepidoptera: nolidae). *Micron* 140, 102957.
- Renthal, R., Velasquez, D., Olmos, D., Hampton, J., Wergin, W.P., 2003. Structure and distribution of antennal sensilla of the red imported fire ant. *Micron* 34, 405–413.
- Rubinoff, D., 2006. Utility of mitochondrial DNA barcodes in species conservation. *Conserv. Biol.* 20 (4), 1026–1033.
- Ruchty, M., Romani, R., Kuebler, L.S., Ruschioni, S., Roces, F., Isidoro, N., Kleineidam, C.J., 2009. The thermo-sensitive sensilla coeloconica of leaf-cutting ants (*Atta vollenweideri*). *Arthropod Struct. Dev.* 38 (3), 195–205.
- Saitou, N., Nei, M., 1987. The neighbor-joining method: a new method for reconstructing phylogenetic trees. *Mol. Biol. Evol.* 4, 406–425.
- Santschi, F., 1920. Quelques nouveaux Camponotinae d'Indochine et Australie. *Bull. Soc. Vaudoise Sci. Nat.* 52, 565–569.
- Schneider, D., 1964. Insect antennae. *Annu. Rev. Entomol.* 9, 103–122.
- Shanbhag, S.R., Sing, K., Singh, R.N., 1995. Fine structure and primary sensory projections of sensilla located in the sacculus of the antenna of *Drosophila melanogaster*. *Cell Tissue Res.* 282, 237–249.
- Shanbhag, S.R., Müller, B., Steinbrecht, R.A., 1999. Atlas of olfactory organs of *Drosophila melanogaster* 1. Types, external organization, innervation and distribution of olfactory sensilla. *Int. J. Insect Morphol. Embryol.* 28, 377–397.
- Sharma, K.R., Enzmann, B.L., Schmidt, Y., Moore, D., Jones, G.R., Parker, J., Berger, S.L., Reinberg, D., Zwiebel, L.J., Breit, B., Liebig, J., 2015. Cuticular hydrocarbon pheromones for social behavior and their coding in the ant antenna. *Cell Rep.* 12 (8), 1261–1271.
- Tamura, K., Nei, M., Kumar, S., 2004. Prospects for inferring very large phylogenies by using the neighbor-joining method. *Proc. Natl. Acad. Sci. Unit. States Am.* 101, 11030–11035.
- Tominaga, Y., Yokohari, F., 1982. External structure of the sensillum capitulum, a hygroreceptive and thermoreceptive sensillum of the cockroach, *Periplaneta americana*. *Cell Tissue Res.* 226, 309–318.
- van Baaren, J., Boivin, G., Bourdais, D., Roux, O., 2007. Antennal sensilla of hymenopteran parasitic wasps: variations linked to host exploitation behavior. *Mod. Res. Educ. Top. Microsc.* 1, 345–352.
- Wachkoo, A.A., Bharti, H., Akbar, S.A., 2020. Taxonomy and geographic distribution of the ant genus *Odontoponera* Mayr, 1862 (Hymenoptera: Formicidae) in India. *Entomologist's Mon. Mag.* 156 (4), 245–252.
- Wheat, C.W., Watt, W.B., 2008. A mitochondrial-DNA-based phylogeny for some evolutionary-genetic model species of *Colias* butterflies (Lepidoptera, Pieridae). *Molecular Phylogenetics and Evolution* 47 (3), 893–902.
- Williams, S.T., Knowlton, N., 2001. Mitochondrial pseudogenes are pervasive and often insidious in the snapping shrimp Genus *Alpheus*. *Molecular Biology and Evolution* 18 (8), 1484–1493.
- Waugh, J., 2007. DNA barcoding in animal species: progress, potential and pitfalls. *Bioessays* 29 (2), 188–197.
- Yamane, S., 2009. *Odontoponeradenticulata* (F. Smith) (Formicidae: Ponerinae), a distinct species inhabiting disturbed areas. *ARIES* 32, 1–8.
- Yang, H., Yan, S.C., Liu, D., 2009. Ultrastructural observations on antennal sensilla of *Coleophora obducta* (Meyrick) (Lepidoptera: coleophoridae). *Micron* 40, 231–238.
- Zacharuk, R.Y., 1985. Antennae and sensilla. In: Kerkut, G.A., Gilbert, L.I. (Eds.), Comprehensive Insect Physiology, Biochemistry and Pharmacology. Pergamon Press, London, pp. 1–70.